Study of Lepton Jets in ATLAS

Matthew Low

CERN
CH-1211 Genève 23
Switzerland

September 9, 2009

Abstract

A theory of dark matter has been proposed that predicts that highly collimated groups of leptons, "lepton jets", will be seen at the LHC. The theory describes a dark gauge sector consisting of dark matter particles and dark gauge bosons. A Monte Carlo simulation was written to simulate dark gauge boson decays into leptons. These decays were studied in detail and it was determined that any event seen by the ATLAS detector will be very highly collimated. In the case where there are multiple pairs of leptons, these pairs are also highly collimated and, for the values used in the simulation, form a single jet. In the solenoidal magnetic field of ATLAS the leptons can curve closer together or further apart. The separation distribution is composed of both cases in equal quantity and is therefore largely unaffected by the magnetic field. The separations observed are, in general, sufficiently far apart that ATLAS can distinguish leptons within a given jet simply from geometry. It was also found that from the detected leptons it is straightforward to reconstruct the dark gauge boson masses in both the single pair and multiple pair cases.

1 Introduction

Soon the LHC will be operating and providing us with the means to push the energy frontier to levels previously unacheived by any machine. As the LHC has been many years in the making, theorists have had an abundance of time to create theories of what new physics may be seen at these energy scales. While many theories have enough free parameters that they can be fit to what is found at the LHC, the collider will nonetheless provide the necessary data to reject a number of theories and steer others in the appropriate direction. It is at the LHC that theory and experiment will get a chance to advance together, giving insight into the nature of our world.

Among these recently developed theories include some that go as far as to characterize dark matter in terms of gauge symmetries and make predictions about how it will manifest itself at the LHC. One of these theories predicts that highly collimated groups of leptons, or "lepton jets", will be seen at the LHC. This paper presents a Monte Carlo simulation that was written to investigate the kinematics of these lepton jets in the ATLAS detector.

2 Theory

In recent years there have been a number of anamolous results from several different astrophysics experiments. In particular: PAMELA (A Payload for Antimatter Matter Exploration and Light-nuclei Astrophysics) has found an excess in the positron fraction ($e^+/(e^+ + e^-)$) in the energy range of $10-100$ GeV; ATIC (Advanced Thin Ionization Calorimeter) cannot distinguish between electrons and positrons but has found an excess of $e^+ + e^-$ in the energy range of $300 - 800$ GeV; WMAP (Wilkinson Microwave Anisotropy Probe) has found there are high-energy emissions from galatic centers which are unaccounted for; and EGRET (Energetic Gamma-Ray Experiment Telescope) has found a gamma ray excess in the energy range of $10 - 50$ GeV.

While it is true that each result can be explained via a different phenomenon, Arkani-Hamed et al. have proposed a theory that explains all of the results in a very unified fashion [1]. The theory introduces a new dark gauge sector which accounts for the the presence of dark matter in the universe and the astrophysics results cited above. In this framework, the dark matter itself consists of heavy dark matter particles on the order of $500 - 800$ GeV, and light dark gauge bosons on the order of ≈ 1 GeV. The high mass of the dark matter particles is in accord with the calculated presence of dark matter in the universe. The low mass of the gauge bosons provides two key aspects for the theory. The first is that decays to protons are supressed purely from kinematics, thus favouring leptonic decays to electrons[1], and muons. The second is that the leptonic cross section is increased via the Sommerfeld enhancement. This allows the cross section to be high enough at present to fit the astrophysical data and low enough in the early universe to fit the cosmological data.

The light gauge bosons of the dark sector are predicted to decay via Standard Model particles, and the only kinematically accessible ones are electrons and muons. Since these gauge bosons have a very low mass and are produced in decays of massive dark particles, their lepton products will be boosted and highly collimated. Arkani-Hamed and Weiner give these groups of leptons the name "lepton jets" [2].

While in this theory supersymmetry is not necessary, several theorists argue that it is well

[1] In this paper, electrons and positrons are referred to collectively as electrons.

motivated [3]. In a SUSY version of the dark matter theory the LHC enters the picture because of its high energy. If the LHC reaches a high enough energy to create SUSY particles, then these particles may decay to SUSY particles of the dark sector which in turn will decay in the dark gauge bosons and then into lepton jets. According to Baumgart et al. there is another way these dark gauge bosons can be produced that does not require SUSY, namely direct production.[2] This arises due to a small kinetic mixing between the dark force carrier and the Standard Model photon. Consequently Standard Model electromagnetic fields also contain a small dark charge which would produce these dark gauge bosons. In this case it is the high luminosity of the LHC that provides the discovery potential.

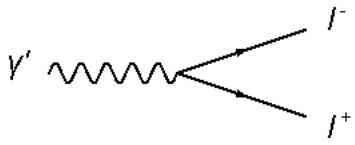

Figure 1: A two lepton decay of the dark gauge boson.

This paper focuses on direct production and studies, in particular, two decay chains predicted by Baumgart et al. Following the notation presented in [3], γ' represents a dark gauge boson, and w' represents another dark gauge boson which couples to the γ'. The first decay, a two lepton decay can be seen in Figure 1. The second is a four lepton decay, as seen in Figure 2, and only arises since the dark matter theory they present is non-abelian. As such they also present decay chains including six and eight leptons, but these were not studied in this paper.

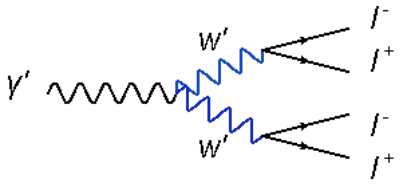

Figure 2: A four-lepton decay of the dark gauge boson.

The kinematics of these decays can be studied by simply specifying the appropriate four-vector distributions; it is not necessary to simulate the production mechanism.

3 Simulation

While there exist several software packages for the simulation of physics processes[3], the software for the simulation was written in its entirety using only C++ libraries. This served several purposes: while it was primarily a pedagogical exercise, it also provided a fast way to generate events. The software package used to analyze the simulated data was ROOT[7].

[2]This is very similar to prompt photon production in the Standard Model [3].
[3]Such as ATHENA, PYTHIA, ALPGEN, etc.

3.1 Monte Carlo Methods

In order to simulate the physics processes involved in a theory of dark matter it was necessary to create a framework capable of producing random variables according to specified distributions. Two general distributions that were frequently used were a uniform random distribution and a Gaussian random distribution. The uniform random distribution was generated by using the C++ `rand()` function and scaling and shifting it as necessary. The Gaussian random distribution was generated using the Box-Muller Transform[4]. The essence of the method is to choose two random numbers x_1 and x_2, uniform from 0 to 1, and transform them as:

$$x_1' = \sqrt{-2\ln x_1}\cos 2\pi x_2 \quad (1)$$

$$x_2' = \sqrt{-2\ln x_1}\sin 2\pi x_2 \quad (2)$$

into two Gaussian random numbers x_1' and x_2'. In the simulation, the polar form of the Box Muller transform was used since it is faster in general. The polar form takes two random numbers x_1 and x_2, uniform from -1 to 1, and computes $r^2 = x_1^2 + x_2^2$. If $r^2 > 1$ then x_1 and x_2 are redrawn until they satisfy $r^2 \leq 1$. Then x_1 and x_2 as:

$$x_1' = \sqrt{\frac{-2\ln r^2}{r^2}}x_1 \quad (3)$$

$$x_2' = \sqrt{\frac{-2\ln r^2}{r^2}}x_2. \quad (4)$$

In addition to these commonly used distributions it was necessary to produce distributions according to a generic function $f(x)$. This was done according to the Inverse Transform Sampling method[5]. The method requires $f(x)$ to be integrable and for the integral to be invertible. In cases where the integral was not analytically invertible, it was inverted numerically.

3.2 Event Generation

Using the theory of dark matter, Baumgart et al. presented several concrete models of dark gauge boson decays to Standard Model particles [3]. In particular they provide a plot of the differential cross section of the γ' versus its transverse momentum. The distribution of transverse momentum, p_T, was approximated as,

$$f(p_T) = \frac{\lambda^2}{2}\exp(-\lambda\sqrt{p_T}), \quad (5)$$

where $\lambda = 1.08\ \text{GeV}^{-1/2}$ was measured from the plot in [3]. The resulting plot is shown in Figure 3. Then four-vectors were generated for the γ' using $f(p_T)$ as the transverse momentum distribution. The other required parameters, the azimuthal angle ϕ and the pseudorapidity η, were produced according to typical particle production at hadron colliders. As such, ϕ was uniform between 0 and 2π and η was uniform between -2.5 and 2.5.[6] These four-vectors were then decayed according

[4]The details and proof of this method are beyond the scope of this paper but can be found at http://en.wikipedia.org/wiki/Box-Muller_transform.

[5]The details of this method are beyond the scope of this paper but can be found at http://en.wikipedia.org/wiki/Inverse_transform_sampling.

[6]The η limits are the bounds of the ATLAS Inner Detector.

Particle	Monte Carlo Code	Mass (GeV)
γ'	601	1.5
w'	602	0.6
$e^{\pm}$	$\pm$11	0.000510998910
$\mu^{\pm}$	$\pm$13	0.105658367

Table 1: Masses used in the simulation taken from Baumgart et al. [6]

to the decays presented in Figures 1 and 2. The mass values used can be found in Table 1. These are the same values used in the Monte Carlo used by Baumgart et al. The two-lepton decay produces either an electron and a positron or two muons, while the four lepton decay produces two electrons and two positrons or four muons from a pair of w's. These decays were produced spherically uniform[7] in the rest frame of the γ' and then the lepton four-vectors were boosted back into the lab frame. The four-vectors of the boosted leptons were used to derive various kinematic variables which were analyzed in detail.

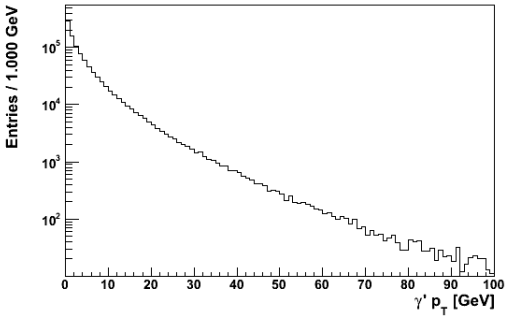

Figure 3: The γ' cross section produced from Equation 5.

3.3 Trigger Requirement

Inside the LHC there will be bunch crossings every 25 ns. This will produce more collisions than seen before in any other experiment to date. Each collision will take about 1.5 Mb of disk space so storing this amount of data is unfeasible. As it turns out many of the collisions are "uninteresting" background processes and will not need to be stored. In order to make fast decisions on which events to store, ATLAS employs a trigger system to discriminate between events. This means that not all events will be recorded, depending on whether or not they meet the requirements as decided by the ATLAS Trigger Menu.

To gain a basic understanding of the effect this would have on the potential to detect and record the lepton jet events, a loose trigger requirement was applied to the simulated data. The

[7]While a spherically uniform decays assumes a scalar gauge boson, other distributions were also simulated with $\cos^2(\theta)$ and $\sin^2(\theta)$ dependences for a vector gauge boson. While the shape of some distributions were slightly modified, the kinematics remained unchanged.

lepton products of the generated γ' were required to include one electron with $p_T > 12$ GeV[8], or one muon with $p_T > 10$ GeV, or two electrons with $p_T > 5$ GeV, or two muons with $p_T > 4$ GeV.

In addition to the trigger requirement, an inner detector requirement was also applied. This requirement was used to simulate the limits of the particles that the ATLAS detector can detect. The inner detector requirement required all leptons in the event have $p_T > 1$ GeV and $\eta < |2.5|$.

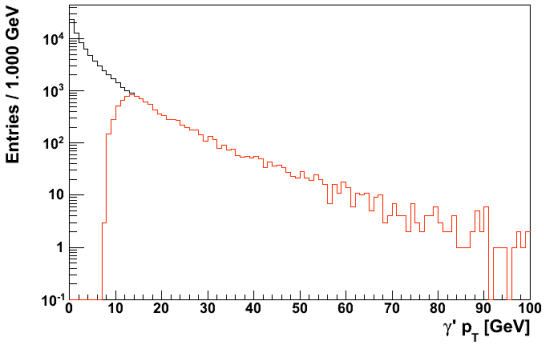

Figure 4: The γ' cross section produced from Equation 5. The black curve is the same as in Figure 3, the red curve is after the trigger requirement and inner detector requirements have been applied.

3.4 Particle Trajectories

In an effort to completely understand the kinematics behind the leptons jets, the particle trajectories were also plotted. It is important to note that the trajectories created are the truth trajectories and not the reconstructed tracks. Also, the trajectories are plotted under the simplifying assumptions that the solenoidal, toroidal, and end-cap toroidal magnetic fields are uniform and that there are no material effects or multiple scattering.

To create the trajectories, the variables needed from each lepton were the charge and the four-momentum. It was also necessary to specify the magnetic field. Then the position $\vec{x_i}$ and momentum $\vec{p_i}$ were propagated according to their current values and the specified magnetic field. The momentum $\vec{p_i}$ was rotated according to the particle's radius of curvature which can be determined as[9]

$$p_T = 0.3zBr \Rightarrow r = \frac{p_T}{0.3zB}, \tag{6}$$

where p_T is the transverse momentum in units of GeV, z is the charge magnitude in units of e, B is the magnetic field in units of Tesla, and r is the radius of curvature in units of metres.

The plotted trajectories allowed a visual inspection of events to verify their plausibility and to gain an intuitive understanding of particle dynamics in the ATLAS magnetic field. Figures 5 and 6 show the electron trajectories in the detector. The electron trajectories were used in the

[8]These values are from a trigger menu presented in the ATLAS CSC book for a luminosity of 10^{31} cm^{-2}s^{-1} [4]. While this is not the nominal luminosity, it will likely be similar to the luminosity at start-up. In any case, the values are sufficient to provide an understanding of the trigger effect.

[9]Equation 6 can easily be derived from the Lorentz force law $\vec{F} = q(\vec{v} \times \vec{B})$ and Newton's law applied to circular acceleration $\vec{F} = m\vec{a_c}$.

analysis to check against other methods. The muon trajectories, as seen in Figures 7 and 8, were created primarily for visual interest.

3.5 Momenta Smearing

In simulations it is possible to maintain the true trajectories and momenta of the various detected particles, however during the actual experiment this is not possible. The granularity of each detector element is finite and thus can only identify a particular value within a finite range with a specified uncertainty. There are also interactions between the particle and the detector material, such as multiple scattering, which can alter the trajectory. To fully emulate the detector's response to an event, it is necessary to simulate each possible interaction between the particles and the detector. However, simulating this is very complex and takes a long time, so quicker approximations can be used if they produce a sufficiently close result. To make this type of simulation, the momenta of the particles can be smeared in a given coordinate system according to Gaussian distributions. Using this technique, the standard deviation of a variable x is given by Equation 7[4], which depends on the particle's transverse momentum:

$$\sigma_x(p_T) = \sigma_x(\infty) \left(1 \oplus \frac{p_x}{p_T}\right) \tag{7}$$

where $\oplus$ stands for addition in quadrature. Also, the values of $\sigma_x(\infty)$ and p_x depend on η and are given by Tables 2 and 3. At high p_T the second term of Equation 7 becomes negligible and it reduces to:

$$\sigma_x(p_T) = \sigma_x(\infty). \tag{8}$$

Therefore $\sigma_x(\infty)$ is from the uncertainty in determining the curvatuve of a particle which is the primary source of uncertainty at high p_T. At low p_T, the first term of Equation 7 becomes negligible and the equation reduces to:

$$\sigma_x(p_T) = \sigma_x(\infty)\frac{p_x}{p_T}. \tag{9}$$

Then Equation 9 is the spread from multiple scattering which is the primary source of uncertainty at low p_T.

Track Parameter	$\sigma_x(\infty)$	p_x (GeV)
Inverse Transverse Momentum (q/p_T)	0.34 TeV^{-1}	44
Azimuthal Angle (ϕ)	70 μrad	39
Polar Angle ($\cot\theta$)	0.7×10^{-3}	5.0

Table 2: From the ATLAS CSC Studies book for $0.25 < |\eta| < 0.50$ [4].

The values from Tables 3.5 and 3.5 were linearly interpolated to provide values for all η. The variables in the table were also put into differential form to find the standard deviation in term

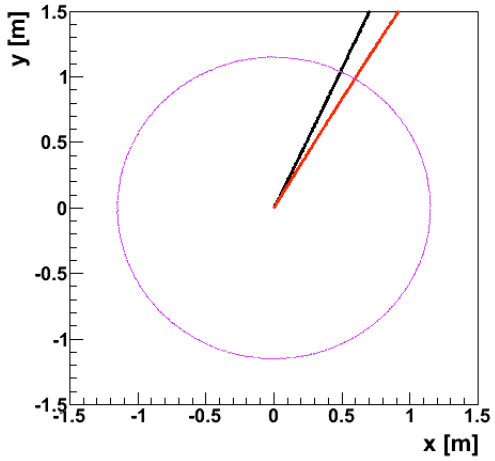

Figure 5: Electron and positron trajectories in the xy-plane. The violet circle is the outer radius of the inner detector at $r = 1.15$ m.

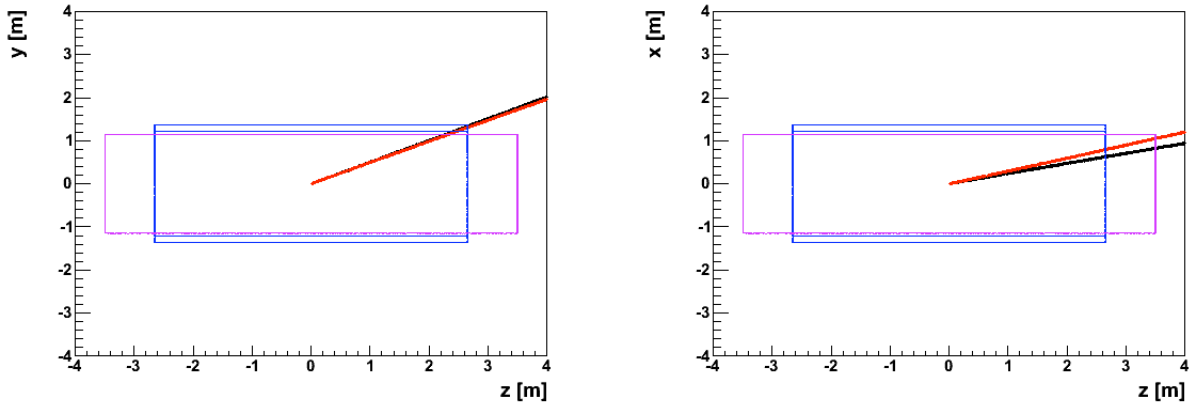

Figure 6: Electron and positron trajectories in the xz-plane and yz-plane. The violet rectangle is the outer radius of the inner detector at $r = 1.15$ m. The blue rectangles are the central solenoid at radii $r_{in} = 1.22$ m and $r_{out} = 1.365$ m.

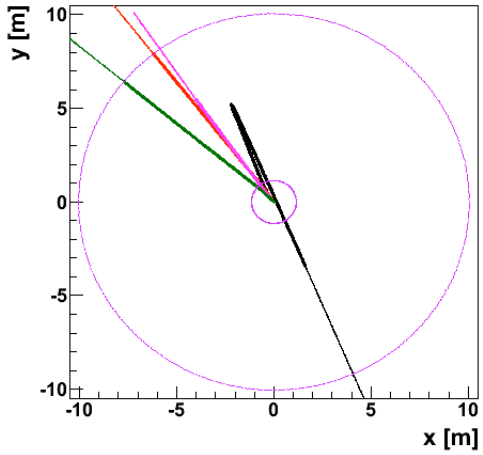

Figure 7: Muon trajectories in the xy-plane. The large violet circle is the outside of the barrel toroids at $r = 10.05$ m and the small violet circle is the outer radius of the inner detector at $r = 1.15$ m.

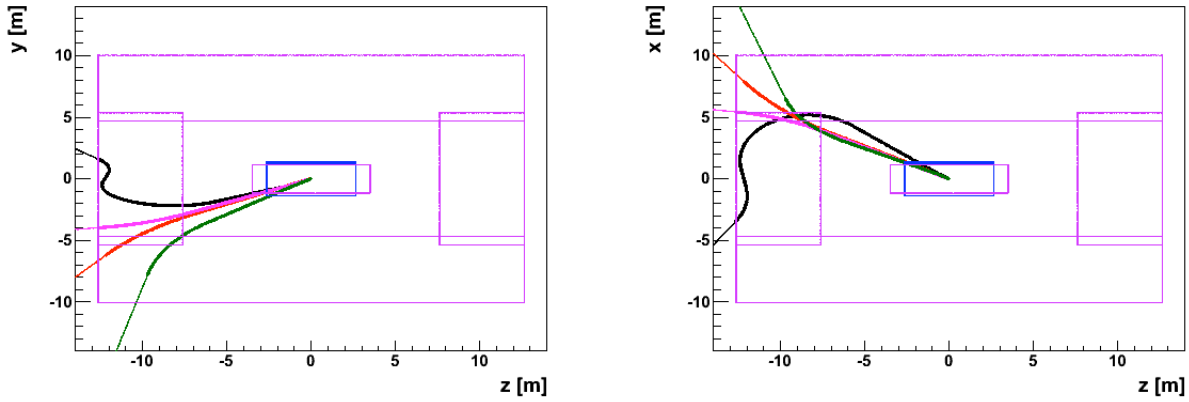

Figure 8: Muon trajectories in the xz-plane and yz-plane. The small violet rectangle is the outer radius of the inner detector at $r = 1.15$ m. The small blue rectangles are the central solenoid at radii $r_{in} = 1.22$ m and $r_{out} = 1.365$ m. The large violet rectangles on the top and bottom are the barrel toroids at $r = 10.05$ m. The large violet rectangles on the left and right are the end-cap toroids at radii $r_{in} = 0.825$ m and $r_{out} = 5.35$ m.

Track Parameter	$\sigma_x(\infty)$	p_x (GeV)
Inverse Transverse Momentum (q/p_T)	0.41 TeV^{-1}	80
Azimuthal Angle (ϕ)	92 μrad	49
Polar Angle ($\cot\theta$)	1.2×10^{-3}	10

Table 3: From the ATLAS CSC Studies book for $1.50 < |\eta| < 1.75$ [4].

of p_T, ϕ, and θ resulting in the following equations:[10]

$$\sigma(p_T) = p_T^2 \sigma\left(\frac{1}{p_T}\right), \tag{10}$$

$$\sigma(\theta) = \sin^2\theta\sigma(\cot\theta), \tag{11}$$

$$\sigma(\phi) = \sigma(\phi). \tag{12}$$

The momentum of the particle is stored in cartesian coordinates $\langle p_x, p_y, p_z\rangle$, which were converted into $\langle p_T, \phi, \theta\rangle$, smeared using the standard deviations according to Equations 12 to yield $\langle p'_T, \phi', \theta'\rangle$, then converted back into cartesian coordinates $\left\langle p'_x, p'_y, p'_z\right\rangle$. These values were then used to determine the energy assuming that the particle type (and thus the mass) is known.

$$E' = \sqrt{m^2 + p_x'^2 + p_y'^2 + p_z'^2} \tag{13}$$

Now the resulting particle four-vectors are appropriately distributed as would be seen in the actual detector. It is also important to mention that the γ' mass distribution prior to smearing was a delta function as was the w' mass distribution.

4 Analysis

While writing the entire Monte Carlo was a useful exercise, it was the analysis of the resulting distributions that provided insight into new physics.

4.1 Opening Angle

One of the primary aspects of the dark matter theory is that the decay of the dark matter gauge bosons will result in lepton jets. To determine if the resulting leptons can justifiably be labelled a jet, it is necessary to examine the opening angle of the leptons.

4.1.1 Two Lepton Decays

In the two lepton case, when the leptons are produced in the γ' rest frame they are always back to back to conserve momentum. Therefore the opening angle in the rest frame of the γ' is always π.[11] However, if the γ's are boosted in the lab frame, the opening angle tends to get smaller because the longitudinal component of the lepton momenta become larger while the tranverse

[10] The following condenses the notation from $\sigma_x(p_T)$ to $\sigma(x)$ and it is assumed that all are functions of p_T.

[11] All opening angles mentioned will be measured in radians.

component remains unchanged. The distribution is shown in Figure 9(a). Figure 9(b) shows the cosine of the same opening angle distribution. It is very interesting to note that the application of the trigger requirement selects only leptons with a very small opening angle, effectively selecting lepton jets. This is because the γ' has a small mass, therefore in order to pass the p_T trigger requirement, it will need to have a larger momentum, resulting in a larger boost between the γ' rest frame and the lab frame. The requirements of the detector itself reinforce the prediction of seeing lepton jets in dark gauge boson decays.

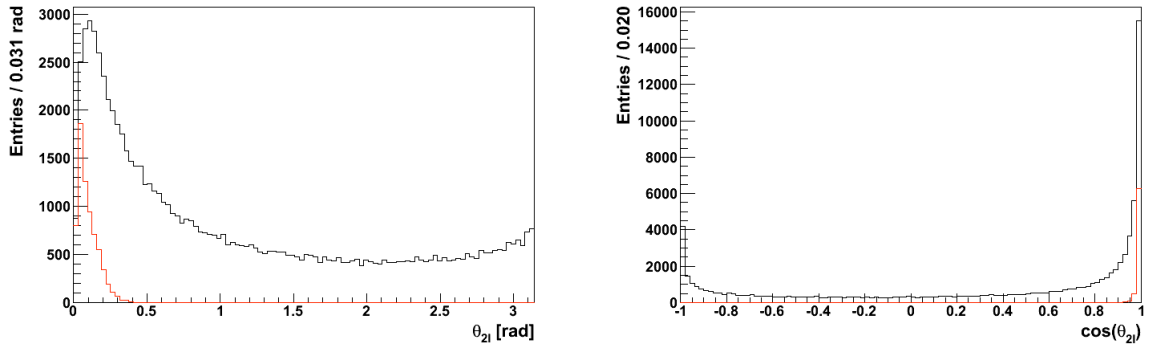

(a) The opening angle between the leptons in a two lepton decay.

(b) The cosine of the opening angle between the leptons in a two lepton decay.

Figure 9: Opening angle distributions of electrons. The black curve is the distribution prior to applying the trigger requirement and the red curve are only the events that pass the trigger requirement.

Figure 10(a) shows the opening angle plotted versus the momentum magnitude of the γ' (after the trigger requirement). Although the plot follows the trend that smaller opening angles correspond to high p_T there are still events that pass the trigger requirement that have a large opening angle and small p_T. It was deduced that these events correspond to situations where the decay is approximately along the direction of flight of the γ'. For these types of events there are two situations that can occur. The first is if $\beta_{\gamma'} < \beta_l$, where $\beta_{\gamma'}$ is the γ' velocity in the lab frame, and β_l is the lepton velocity in the γ' rest frame. In this case, the opening angle remains large after the boost. The second situation that can occur is if $\beta_{\gamma'} > \beta_l$. In this case, the boost flips the direction of one of the leptons so that both leptons are pointing in approximately the same direction in the lab frame, and the opening angle is small. The minimum γ' momentum required to flip the lepton is given by,

$$p_{\gamma'} = \frac{m_{\gamma'}}{2m_l}\sqrt{m_{\gamma'}^2 - 4m_l^2} \tag{14}$$

Inserting the mass values yields $p_{\gamma'} = 2205.9$ GeV for electrons while $p_{\gamma'} = 10.5$ GeV for muons. This agrees with Figure 10(a), as there are events in the first situation since all γ' generated have $p_{\gamma'} \leq 2205.9$ GeV. In the case of muons, any γ' particles with $p_{\gamma'} \leq 10.5$ GeV will not make it past the trigger requirement. Figure 10(b) shows exactly this result, confirming the interpretation.

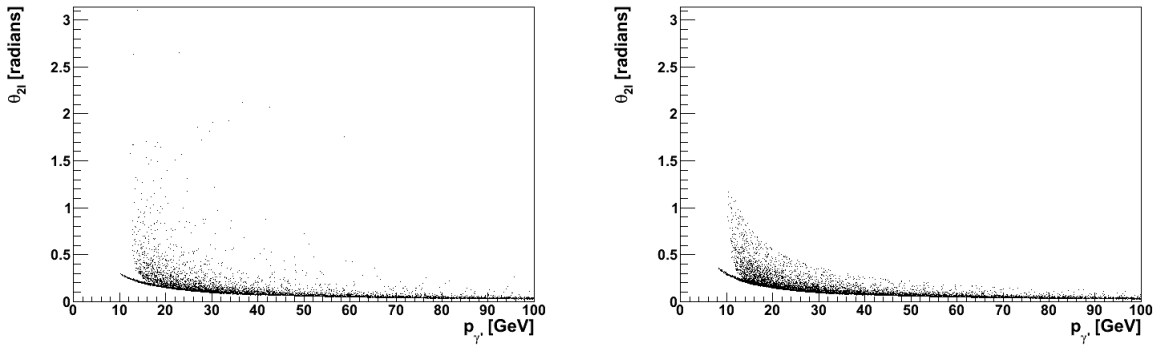

(a) Electrons.

(b) Muons.

Figure 10: Opening angle versus the momentum magnitude of the γ'.

4.1.2 Four Lepton Decays

For each pair of leptons produced from w' decays the kinematics determined in the previous section still apply since the w' is also very light and thus will also be highly boosted. Another question that arises in the analysis of four lepton events that does not come up in the two lepton discussion is whether the four leptons form a single jet of four leptons or form two jets of two leptons. To examine this the opening angle between the two w's was compared to the opening angle between leptons from the same w'. Figure 11 shows the results that $\theta_{w'}$ tends to be smaller than θ_{2l} and in fact comparing event by event it turns out that $\theta_{w'}$ is always smaller. Because of this, the lepton pairs do not have a sufficient separation to become two separate jets so the four-lepton case results in a single lepton jet[12].

4.2 Lepton Separation

In order for these kinematics to be useful, it is necessary that the leptons in a given jet are distinguishable to the ATLAS detector. If this is the case, then lepton jets may make a distinct signal for which to search. Baumgart et al. suggest in their paper that leptons within a given jet are distinguishable based on difference in p_T, however it is difficult to say if the Δp_T in a given jet is sufficiently large to make this distinction. In this study, the lepton separation in the inner detector was examined to see if the lepton separation was greater than the detector resolution and to understand the effect of the magnetic field on the separation.

There are two useful types of lepton separations on the detector. The first is the separation in the xy-plane, essentially disregarding the z-component. This is very useful as it emphasizes the effect of the magnetic field[13] and gives an accurate physical separation in metres as if the inner detector barrel was rolled out flat. The second is the three-dimensional separation. This is useful since it can be used to find the $\Delta\eta \times \Delta\phi$ value to compare to the actual detector values. In terms

[12]This is dependent upon the masses choosen for w'. For instance, if $m_{w'}$ was choosen to be several times smaller then the w's would be produced at a higher momentum and so the component of the lepton boost in the direction of the w' flight would be greater, increasing $\theta_{w'}$.

[13]The magnetic field in the solenoid was approximated to be $\vec{B} = B_z\hat{z}$ where $B_z = 2\text{T}$. According to the Lorentz force law, the direction of the magnetic force is only in the xy-plane.

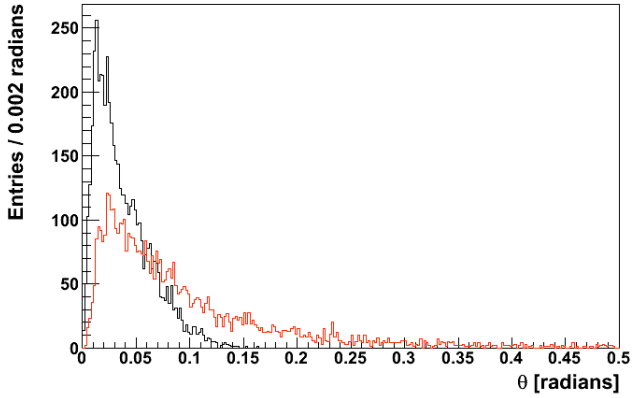

Figure 11: The black curve is $\theta_{w'}$, the opening angle between the w's. The mean of the distribution is 0.0375 rad. The red curve is θ_{2l}, the opening angle between a pair of leptons. The mean of the distribution is 0.0930 rad.

of a physical separation in metres, however, this separation is only an approximation since the inner detector is a cylinder, so the arc length found from the three-dimension separation suffers from the cylinder's non-sphericity.

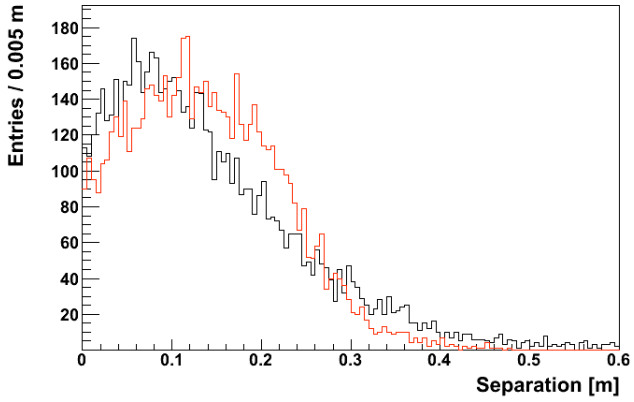

Figure 12: The xy-separation of the leptons at the outer radius of the inner detector, $r = 1.15$ m. The black curve is with the magnetic field and has a mean of 14.0 cm. The red curve is without the magnetic field and has a mean of 14.3 cm.

Figure 12 shows the two lepton xy-separation with and without the magnetic field. Interestingly the magnetic field introduces only a very small effect on the separation. The hypothesized cause for this was the fact that the magnetic field can cause leptons to diverge (curl further away from each other) or converge (curl closer together). Upon analysis it was found that these two possibilities occur with approximately equal frequency. Figure 13 separates the two cases and finds that each case alone produces a significant separation. It is the combination of both of these cases in equal quantity that produces a small net effect from the magnetic field, confirming the

hypothesis. It is also important to note that this effective cancellation is sensitive to the magnetic field strength and the opening angle distribution.

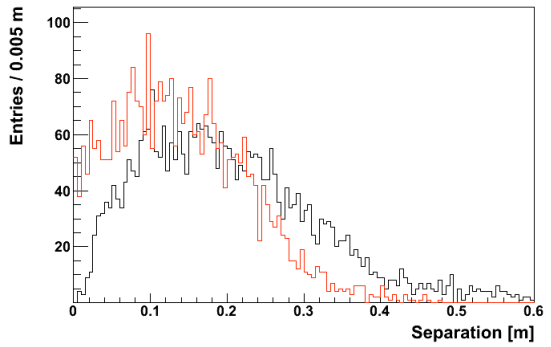

(a) Leptons that curl away from each other in the magnetic field. With the magnetic field the mean is 20.2 cm. Without the magnetic field the mean is 14.1 cm.

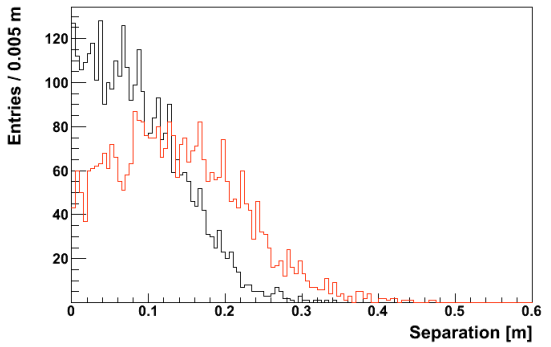

(b) Leptons that curl towards each other in the magnetic field. With the magnetic field the mean is 8.6 cm. Without the magnetic field the mean is 13.7cm.

Figure 13: Lepton separations for leptons that curl away and towards each other separately. The black curve is with the magnetic field and the red curve is without the magnetic field.

In the four lepton case, there four leptons thus by combinatorics there are six possible separations to consider. In Figure 14 the maximum and minimum separations are considered. In the case of the minimum separation, the effect of the magnetic field is small but still noticeable, and for the maximum separation the magnetic field increases the separation very noticeably. The increased effect on the four lepton case is likely due to the fact that there are four leptons sharing the same energy as in the two lepton case. Thus on average the leptons will have less p_T and will curl more due to the magnetic field. Also, while considering the minimum and maximum distances, the effects of convergent and divergent curls are much less pronounced.

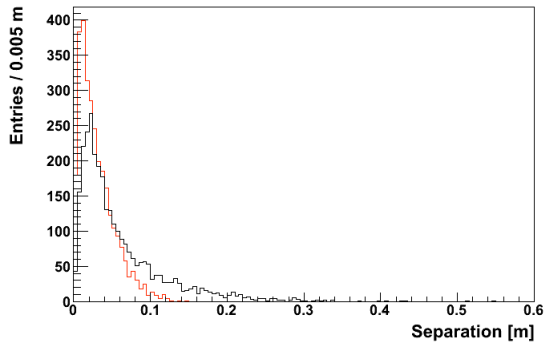

(a) The minimum separation between a pair of leptons. With the magnetic field the mean is 5.99 cm. Without the magnetic field the mean is 3.01cm.

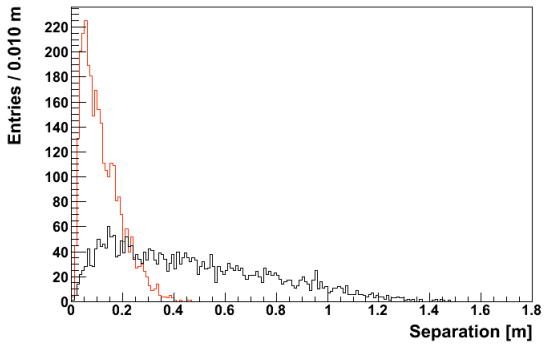

(b) The maximum separation between a pair of leptons. With the magnetic field the mean is 47.14 cm. Without the magnetic field the mean is 11.75cm.

Figure 14: Four lepton separations in the inner detector at $r = 1.15$ m. The black curve is with the magnetic field and the red curve is without the magnetic field.

Source	$\Delta\eta \times \Delta\phi$
Lepton Separation	0.110×0.130
Sampling 1	0.003×0.100
Sampling 2	0.025×0.025
Sampling 3	0.050×0.025

Table 4: The $\Delta\eta \times \Delta\phi$ resolution compared against the electromagnetic calorimeter barrel sampling as stated in the ATLAS TDR [5].

Using the three-dimensional separation the values shown in Table 4 were found. The lepton separation numbers are taken from the means of the $\Delta\eta$ and $\Delta\phi$ distributions. According to the current numbers used by ATLAS, it is likely that the leptons in a given jet can be distinguished based on which detector element they hit.

4.3 Mass Reconstruction

Using the smeared momenta from Section 3.5 it is possible to reconstruct the invariant mass of the γ' particles. This is equivalent to the type of analysis that would be conducted with the actual data to determine the mass of the γ'. This is done by adding the lepton four-vectors and finding the invariant mass of the sum.[14] Figure 15(a) shows the reconstruction for the two lepton case, and Figure 15(b) shows the reconstruction for the four lepton case. In each plot the distribution is a Gaussian centered at approximately 1.5 GeV, as expected.

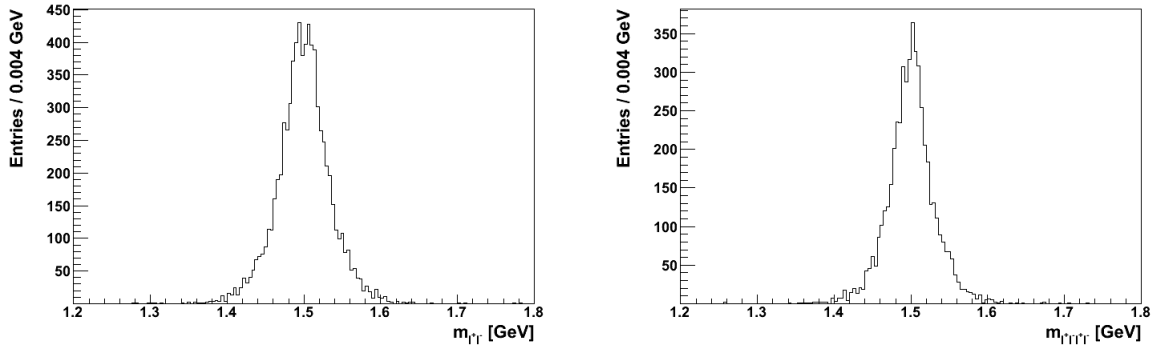

(a) Mass reconstruction of γ' for the two lepton decay. The mean of the distribution is 1.49962 GeV and the RMS is 0.0356731 GeV.

(b) Mass reconstruction of γ' for the four lepton decay. The mean of the distribution is 1.49996 GeV and the RMS is 0.0322522 GeV.

Figure 15: Mass reconstructions of the γ'.

In the four lepton decay there is also an additional complication if one wishes to reconstruct the mass of the w'. There are two pairs of leptons, each with a negatively charged lepton, and a positively charged lepton. When reconstructing the w' mass, it may be difficult to tell which

[14] In particular, if the lepton four-vectors are p_1^μ and p_2^μ then let $p^\mu = p_1^\mu + p_2^\mu$. The invariant mass is simply $(p^\mu)^2 = p_0^2 - \vec{p}^2 = E^2 - \vec{p}^2 = m^2$.

leptons came from the same w' as opposed to mismatching the leptons to different w's. This is a problem since while for each case the distribution is centered at $m_{w'} = 0.6$ GeV (the correct mass), in reconstruction it will not be known which case belongs in which histogram and linear combinations of the two cases may not yield the correct mean. In lieu of this it has been suggested to use the same charge lepton pairs to distinguish the mismatched pair separation [8]. It turns out that the distribution of same charge pairs has the same shape as mismatched pairs and can be "subtracted" from all of the different charge pairs to accurately reconstruct the w' mass. Figure 16 shows these distributions. From the figure it is clear that subtracting these plots would provide a reliable reconstruction of the w' mass.

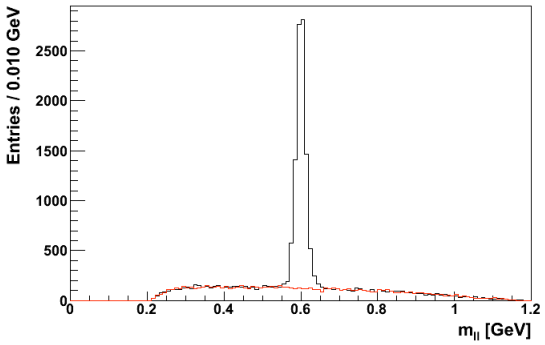

Figure 16: The black curve is all of different charge lepton pairs and the red curve is all of the same charge lepton pairs.

5 Conclusion and Outlook

It was a very useful exercise to write an entire Monte Carlo framework and aided greatly in the understanding of lepton jets. In particular, writing the Monte Carlo allowed for a complete mastery of parameters and assumptions involved in generating the simulated events. Furthermore, although a specific model was used in generating the Monte Carlo, many of the results presented here hold for any model in which a light particle decays to leptons.

It was found that in the two lepton decays of the dark gauge boson, the leptons are highly collimated and so it is justified to call them lepton jets. The requirement dictated by the trigger, even at low luminosities, reinforces the jet structure and only selects leptons with small opening angles. These kinematics apply equally to the four lepton decay. It was also found that for the particular mass values chosen the four leptons create a single lepton jet.

In order to understand the detection potential for the leptons it was necessary to study their separation in the detector and the effect of the solenoidal magnetic field. It was found that in the two lepton case, the magnetic field causes as many leptons to curl together as to curl apart and these effects cancel each other out. The ATLAS detector resolution was also determined to be sufficiently large to separate leptons within a jet based on where they hit the detector.

Lastly, applying the appropriate momenta smearings, it was possible to reconstruct the mass of the γ' as would be seen in the detector. The result was a Gaussian with a mean of 1.5 GeV,

exactly the value input into the Monte Carlo. Reconstructing the mass of the w' was also possible, but required the extra "trick" of subtracting the same charge lepton pairs from the opposite charge lepton pairs. The result was a Gaussian as well, with a mean of 0.6 GeV, the value input into the Monte Carlo.

Future work could include feeding the generated four-momenta into a full detector simulation to see the detector response, or extending the simulation itself to more closely represent the detector. It would also be interesting to use a map of the magnetic field to see the exact trajectories that would be taken by the particles since the capabilities are already present in the code. One particular application that has actually already been discussed would be to use the simulation to probe the parameter space[15] and quickly gain an idea of the new kinematics. At present the Monte Carlo can produce on the order of $50,000$ events in a few seconds and so it has a much shorter turn around time than a full detector simulation without greatly compromising the accuracy of the data.

6 Acknowledgements

I would like to thank Dr. Hulya Guler for supervising me at CERN, and providing direction and guidance, Dr. Andreas Warburton for overseeing my work, and the Institute of Particle Physics along with McGill University for funding me to work at CERN and participate in the CERN Summer Student Program.

[15]For instance, the parameter space of the dark gauge boson masses since there is no reason why $m_{\gamma'}$ should be 1.5 GeV rather than 1.35 GeV.

References

[1] N. Arkani-Hamed, D. P. Finkbeiner, T. Slatyer, and N. Weiner. *A Theory of Dark Matter*, `arXiv:0810.0713` (2008).

[2] N. Arkani-Hamed, and N. Weiner. *LHC Signals for a SuperUnified Theory of Dark Matter*, `arXiv:0810.0714` (2008).

[3] M. Baumgart, C. Cheung, J. T. Ruderman, L. Wang, and I. Yavin. *Non-Abelian Dark Sectors and Their Collider Signatures*, `arXiv:0901.0283` (2009).

[4] The ATLAS Collaboration. *Expected Performance of the ATLAS Experiment, Detector, Trigger and Physics* (2008).

[5] The ATLAS Collaboration. *Technical Design Report* (1999).

[6] C. Amsler et. al. *Review of Particle Physics*. Physical Letters **B 667**, 1 (2008).

[7] *ROOT, A Data Analysis Framework*. `http://root.cern.ch/` (2009).

[8] ATLAS Long-Lived Particles Group Meeting.